Ferromagnetic tunneling junctions at low voltages: Elastic versus inelastic scattering at T=0° K

C. A. Dartora and G. G. Cabrera

Citation: Journal of Applied Physics **95**, 6058 (2004); doi: 10.1063/1.1703825
View online: http://dx.doi.org/10.1063/1.1703825
View Table of Contents: http://scitation.aip.org/content/aip/journal/jap/95/11?ver=pdfcov
Published by the AIP Publishing

Ferromagnetic tunneling junctions at low voltages: Elastic *versus* inelastic scattering at $T=0\,°K$

C. A. Dartora and G. G. Cabrera[a)]
Instituto de Física 'Gleb Wataghin,' Universidade Estadual de Campinas (UNICAMP), C.P. 6165, Campinas 13083-970 SP, Brazil

(Received 5 January 2004; accepted 18 February 2004)

In this article we analyze different contributions to the magnetoresistance of magnetic tunneling junctions at low voltages. A substantial fraction of the resistance drop with voltage can be ascribed to variations of the density of states and the barrier transmission with the bias. However, we found that the *anomaly* observed at zero bias and the magnetoresistance behavior at very small voltages, point to the contribution of inelastic magnon-assisted tunneling. The latter is described by a transfer parameter T^J, which is one or two orders of magnitude smaller than T^d, the direct transmission for elastic currents. Our theory is in excellent agreement with experimental data, yielding estimated values of T^J which are of the order of $T^d/T^J \sim 40$. © *2004 American Institute of Physics.*
[DOI: 10.1063/1.1703825]

I. INTRODUCTION

Recently, the interest in the phenomena of giant magnetoresistance (GMR) in magnetic tunnel junctions (MTJ) has grown significantly due to potential applications in magnetoresistive reading heads, magnetic field sensors, nonvolatile magnetic random access memories, and many others.[1–5] The effect is based on the spin dependent scattering mechanisms proposed in the early papers by Cabrera and Falicov,[6] which lead in MTJ's, to a strong dependence of the conductance on the magnetic polarization.[7] Typically, the GMR effect found in MTJ's is of the order of 25%–30%,[8,9] and points to a large ratio of the densities of states for majority (M) and minority (m) electrons at the Fermi level (E_F)

$$\frac{N_M(E_F)}{N_m(E_F)} \approx 2.0-2.5.$$

As usual in MR experiments, one compares the resistances for the cases where the magnetizations at the electrodes are antiparallel (AP) and parallel (P). In several experiments reported in the literature (see for example Refs. 1, 2, 8, and 9), the junction resistance drops significantly with the applied voltages, with a sharp peak at zero bias (*zero-bias anomaly*). This bias dependence shows a rapid initial decrease up to voltages of the order of $V \sim 100$ mV, then slows down but continues decreasing with voltages, up to 60% of the peak value at 500 mV in some cases.[9] Many attempts to explain the above behavior have been done over the last years,[1,2,8,10] but a complete theory which includes all the observed features is still lacking.

In Ref. 8, scattering from magnons at the electrode-insulator interface has been proposed as the mechanism for randomizing the tunneling process and opening the spin-flip channels that reduce the MR. While this process may explain the MR behavior in the vicinity of zero-bias (voltages smaller than 40–100 mV), estimations of magnon scattering cross sections show that the effect is too small to account for the sharp drop in resistance observed in the whole range of 500 mV. In fact, inelastic-electron tunneling spectroscopy (IETS) measurements at low temperature showed peaks which can unambiguously be associated with one-magnon spectra at very small voltages (from 12 to 20 mV, with tails up to 40 mV, and maximum magnon energy not larger than 100 meV).[1] To go beyond this limit will imply multimagnon processes, which are negligible at low temperature. This way, the electron-magnon coupling constant coming from Ref. 8 is by sure considerable overestimated.

The above explanation[8] has been challenged in Ref. 10, where it is shown that the experimental data can be understood in terms of elastic tunneling currents which conserve spin, by considering effects not taken into account in Ref. 8. Those include the lowering of the effective barrier height with the applied voltage, as in the classical Simmons' theory,[11] and most important, variations of the densities of states with the bias at both magnetic electrodes. The latter is a relevant question, since experiments probe depths of the order of 0.5 eV from the Fermi surface. The simple calculation developed in Ref. 10 models the band structure with free electron-like densities of states, since the tunneling current is dominated by the *s*-electron contribution. This approach yields a *zero bias* anomaly which depends on the band structure, and a variation of the MR which has the right order of magnitude for the whole range of 500 meV. The above discussion and other experimental results primarily exhibit that the density of states dependence on the applied voltage plays an important role.[12,13] However, fine details of experiments at very small voltages are difficult to fit. One may adopt here a pragmatic procedure, with a more intricate band structure and more free parameters to improve the fitting.[2]

In this article we take a different stand, motivated by results from IETS experiments,[1] which show that inelastic scattering do participate in the phenomenon at very small voltages. Also, MR experiments[8,9] show clearly a different behavior with applied voltage in the same small bias region

a)Electronic mail: cabrera@ifi.unicamp.br

(up to 100 mV). A complete theory then should include:

(i) Magnon assisted tunneling effects, with maximum magnon energies of the order of ~100 meV. At low temperature, electrons from the electrodes, accelerated by the applied voltage, excite magnons at the interface. At low temperature, only magnon-emission processes should be considered;
(ii) Variation with voltages of the densities of states for the different spin bands in the ferromagnets. Here, we will follow closely the approach of Ref. 10, with a simple picture of the band structure. This is motivated by the discussions given in Refs. 14 and 10 over the polarization of the tunneling current. We assume here that the latter is mainly of *s*-character;
(iii) Lowering of the effective barrier height with the applied voltage. This effects, as shown in Ref. 11, yields to a parabolic dependence of the resistance with the bias. It does not contribute to the *zero-bias* anomaly, but it is always present and should dominate the behavior at large voltages.

The above program will be developed in the present contribution. The content of this paper can be described as follows: In the next section, we formulate the theoretical basis for analyzing tunneling currents, discussing the transfer Hamiltonian which includes all the above mentioned ingredients. In Sec. III, we solely analyze density of states effects, considering elastic tunneling processes. Some analytical expressions are shown. In Sec. IV, we include contributions from inelastic magnon-assisted processes to the tunneling current, and finally, in the last section, a few conclusions and remarks are added.

II. THEORETICAL PRELIMINARIES

To give a description of the MR and the resistance in the MTJ, we will use the transfer Hamiltonian method.[15] The junction is composed by two ferromagnetic electrodes separated by a thin oxide film which represents a potential barrier due to the fact that the Fermi levels of the ferromagnetic layers are situated in the gap region of the oxide film. We have considered the *s*-band electrons as free particles (plane-waves), being responsible for the dominant contribution to the tunneling process. The *d* electrons, which are more localized, enter in the process only via the exchange interaction with *s* electrons on each ferromagnetic electrode. In the context of second quantization and neglecting the magnetization energy (Zeeman term), the unperturbed Hamiltonian is given by

$$H_0=\sum_{\mathbf{k}\sigma,\alpha=(L,R)} E_{\mathbf{k}\sigma} c^{\alpha\dagger}_{\mathbf{k}\sigma} c^{\alpha}_{\mathbf{k}\sigma} \tag{1}$$

with $L(R)$ referring to the left (right) ferromagnetic electrode, $c^{\alpha\dagger}_{\mathbf{k}\sigma}$ ($c^{\alpha}_{\mathbf{k}\sigma}$) are the creation (annihilation) fermionic operators for wave vector $\mathbf{k}$ and spin σ, $E_{\mathbf{k}\sigma}=\hbar^2k^2/2m-\sigma\Delta_\alpha$ is the Hartree–Fock energy, and Δ_α is the shift in energy due to exchange interaction in each side of the barrier.

In writing the interaction part of the total Hamiltonian, which makes possible the transfer of electrons from one side of the insulating barrier to the other, we follow Ref. 8. Apart from the direct transfer which comes from elastic processes, we include transfer with magnetic excitations that originates from the *s-d* exchange between conduction electrons and localized spins at the interfaces. The excitations are described by a linearized Holstein–Primakoff transformation,[16] in the spirit of a one-magnon theory. We use the following Hamiltonian:

$$\begin{aligned} H_{\mathrm{int}}=&\sum_{\mathbf{k}\mathbf{k}'\sigma} t^{d}_{\mathbf{k}\mathbf{k}'}(c^{L\dagger}_{\mathbf{k}\sigma}c^{R}_{\mathbf{k}'\sigma}+c^{R\dagger}_{\mathbf{k}'\sigma}c^{L}_{\mathbf{k}\sigma}) \\ &+\frac{1}{\sqrt{N_s}}\sum_{\mathbf{k}\mathbf{k}'\mathbf{q}} t^{J}_{\mathbf{k}\mathbf{k}'\mathbf{q}}(c^{L\dagger}_{\mathbf{k}\downarrow}c^{R}_{\mathbf{k}'\uparrow}+c^{R\dagger}_{\mathbf{k}'\downarrow}c^{L}_{\mathbf{k}\uparrow})(\sqrt{2S_L}b^{L}_{\mathbf{q}} \\ &+\sqrt{2S_R}b^{R}_{\mathbf{q}})+\frac{1}{\sqrt{N_s}}\sum_{\mathbf{k}\mathbf{k}'\mathbf{q}} t^{J}_{\mathbf{k}\mathbf{k}'\mathbf{q}}(c^{L\dagger}_{\mathbf{k}\uparrow}c^{R}_{\mathbf{k}'\downarrow}+c^{R\dagger}_{\mathbf{k}'\uparrow}c^{L}_{\mathbf{k}\downarrow}) \\ &\times(\sqrt{2S_L}b^{L\dagger}_{\mathbf{q}}+\sqrt{2S_R}b^{R\dagger}_{\mathbf{q}})+\frac{1}{N_s}\sum_{\mathbf{k}\mathbf{k}'\mathbf{q}} t^{J}_{\mathbf{k}\mathbf{k}'\mathbf{q}}(c^{L\dagger}_{\mathbf{k}\uparrow}c^{R}_{\mathbf{k}'\downarrow} \\ &-c^{L\dagger}_{\mathbf{k}\downarrow}c^{R}_{\mathbf{k}'\downarrow}+h.c.)[S_L+S_R-(b^{R\dagger}_{\mathbf{q}}b^{R}_{\mathbf{q}}+b^{L\dagger}_{\mathbf{q}}b^{L}_{\mathbf{q}})], \end{aligned} \tag{2}$$

where $t^{d}_{\mathbf{k}\mathbf{k}'}$ is the direct transmission coefficient, $t^{J}_{\mathbf{k}\mathbf{k}'\mathbf{q}}$ is the inelastic transmission coefficient (depends on the exchange integral), $S^L(S^R)$ is the spin value at the left (right) side, N_s is the total number of spins at the interface, and $b^{\alpha\dagger}_{\mathbf{q}}$ ($b^{\alpha}_{\mathbf{q}}$) are the creation (annihilation) operators for magnons with wave-vector $\mathbf{q}$ at each interface between the barrier and the electrodes. The wave-vector $\mathbf{q}$ is quasi-two-dimensional (the magnon wave function is localized at the interfaces, but with finite localization length).

In general, the total current obtained with Eq. (2) has contributions from elastic processes, resulting in a direct tunneling which conserves spin, and from the inelastic ones, which involve emission and absorption of magnons with electronic spin flip. In the following we describe the direct term.

III. DIRECT TUNNELING CURRENT: ANALYTICAL EXPRESSIONS

Considering only the direct part of the tunneling process, which means elastic processes, without involving magnon excitations, the current is easily obtained by[2,3,8,10]

$$\begin{aligned} I_{(C)}=&\frac{2\pi e}{\hbar}\int dE T^{d}(E,V,d,\Phi_0)W_{(C)}(E,V) \\ &\times[f(E-\mathrm{eV})-f(E)] \end{aligned} \tag{3}$$

where

$$W_{(C)}=\sum_{\sigma} N^{R}_{\sigma}(E)N^{L}_{\sigma}(E-\mathrm{eV}) \tag{4}$$

and C denotes the configuration scheme, $C=\mathrm{P}$ for parallel and $C=\mathrm{AP}$ for antiparallel, $f(E)$ is the Fermi–Dirac distribution, and N^{R}_{σ} and N^{L}_{σ} the density of states at the right and left electrodes, respectively. $T^{d}(E,V,d,\Phi_0)=|t^{d}_{kk'}|^2$ is the tunneling coefficient, being a function of the energy E, the

applied voltage V, the thickness of the barrier d, and the barrier height Φ_0. In fact, T^d is a function of the overlap integral between the left and right wave functions inside the barrier region.

The resistance is readily obtained by $R=G^{-1}$, where $G=dI/dV$ is the differential conductance. In the low bias regime, we are interested in voltages smaller than the Fermi energy and only the states near the Fermi level will contribute to the transport, so we can expand the density of states in a Taylor series as follows:

$$N_\sigma^\alpha(E)=\sum_{n=0}^{\infty}\frac{1}{n!}\frac{d^nN_\sigma^\alpha(E)}{dE^n}\bigg|_{E_F}(E-E_F)^n. \tag{5}$$

Now, let us calculate W_C for the P and AP configurations, using Eq. (5). In the P configuration the majority and minority bands in each electrode corresponds to the same spin orientation, and in AP configuration the majority band of one electrode is the minority on the other

$$W_{(\mathrm{P})}=\sum_i\sum_j\frac{1}{i!j!}\left[\frac{d^iN_M^R(E)}{dE^i}\frac{d^jN_M^L(E-\mathrm{eV})}{d(E-\mathrm{eV})^j}+\frac{d^iN_m^R(E)}{dE^i}\frac{d^jN_m^L(E-\mathrm{eV})}{d(E-\mathrm{eV})^j}\right]\bigg|_{E_F}\times(E-E_F)^i(E-\mathrm{eV}-E_F)^j, \tag{6}$$

and

$$W_{(\mathrm{AP})}=\sum_i\sum_j\frac{1}{i!j!}\left[\frac{d^iN_M^R(E)}{dE^i}\frac{d^jN_m^L(E-\mathrm{eV})}{d(E-\mathrm{eV})^j}+\frac{d^iN_m^R(E)}{dE^i}\frac{d^jN_M^L(E-\mathrm{eV})}{d(E-\mathrm{eV})^j}\right]\bigg|_{E_F}\times(E-E_F)^i(E-\mathrm{eV}-E_F)^j. \tag{7}$$

Taking into account identical electrodes and the low bias regime, we can expand these expressions to first order with good accuracy. The *s*-band can be represented by a parabolic dispersion relation and density of states $N_\sigma\propto\sqrt{E-\Delta_\sigma}$, where $\Delta_\sigma(\sigma=\uparrow,\downarrow)$ gives the bottom of the spin band, with $|\Delta_\uparrow-\Delta_\downarrow|=2\Delta$, as in Ref. 10. However, we consider here cases more general than the parabolic dispersion, with the band structure described through the following set of parameters:

$$r\equiv\left(\frac{N_M}{N_m}\right)_F,\qquad \lambda\equiv\left(\frac{dN_M/dE}{dN_m/dE}\right)_F,\qquad \beta\equiv\left(\frac{1}{N_m}\frac{dN_m}{dE}\right)_F, \tag{8}$$

with all quantities evaluated at the Fermi level, and m and M stand for minority and majority spin bands, respectively. We get the analytic expressions

$$W_{(\mathrm{P})}=(N_m^F)^2\{(1+r^2)+\beta(1+r\lambda)(2\varepsilon-V)+\beta^2(1+\lambda^2)\varepsilon(\varepsilon-V)\}, \tag{9}$$

and

$$W_{(\mathrm{AP})}=(N_m^F)^2\{2r+\beta(r+\lambda)(2\varepsilon-V)+\beta^2\lambda\varepsilon(\varepsilon-V)\}, \tag{10}$$

where $\varepsilon\equiv E-E_F$ and ε and V must be given in eV.

There are several possibilities for including the tunneling transmission coefficient T^d in the theory. One is the approach followed by Simmons,[11] where the barrier is parametrized by an effective height Φ_0 and an effective thickness d

$$T^d(E,V,\Phi_0,d)=\exp\left[-\frac{2}{\hbar}d\sqrt{2m(\Phi_0-\varepsilon_z)}\right]=\exp[-1.024d\sqrt{\Phi_0}]\exp\left[\frac{1}{2}d\frac{\eta\epsilon}{\sqrt{\Phi_0}}\right], \tag{11}$$

where all energies are measured from the Fermi level and given in eV, the barrier width given in angstrom$=0.1$ nm, and η is some constant relating the energy ε with its component ε_z perpendicular to the barrier. This latter parameter appears due to the fact that we are using a one-dimensional (1D) formula to explain the behavior in the 3D case.

Since the Fermi–Dirac functions are step-like at 0°K, we can easily obtain the conductance for both configurations.

$$G_{(C)}=\frac{2\pi e^2}{\hbar}\frac{d}{dV}\left\{\int_0^V d\epsilon T^d(\varepsilon,V,\Phi_0,d)W_{(C)}(\varepsilon,V)\right\}.$$

With some simplifications in the integration process (taking into account the behavior of the integrand in the range of integration, and making use of some geometric arguments), one obtains

$$G_{(C)}=\frac{2\pi e^2}{\hbar}\left\{A_{(C)}T^d(V,\Phi_0,d)+\frac{1}{6}\frac{d}{dV}[B_{(C)}V^2T^d(V,\Phi_0,d)-C_{(C)}V^3T^d(3V/5,\Phi_0,d)]\right\}, \tag{12}$$

where $A_{(C)}$, $B_{(C)}$, and $C_{(C)}$ are constants related to the configuration scheme and the density of states. Following, the analytical expressions for the conductance in both parallel and antiparallel configurations are presented, using Eq. (12) and considering the expansions (9) and (10)

$$G_{(\mathrm{P})}=\frac{2\pi e^2}{\hbar}\exp[-1.024d\sqrt{\Phi_0}][N_m^F]^2 \times\left\{(1+r^2)\exp\left[\frac{\eta Vd}{2\sqrt{\Phi_0}}\right]+\frac{\beta(1+r\lambda)}{3} \times\left[\frac{\eta dV^2}{4\sqrt{\Phi_0}}\exp\left[\frac{\eta Vd}{2\sqrt{\Phi_0}}\right]+V\left(\exp\left[\frac{\eta Vd}{2\sqrt{\Phi_0}}\right]-1\right)\right] -\frac{\beta^2(1+\lambda^2)}{2}\exp\left[\frac{3\eta Vd}{10\sqrt{\Phi_0}}\right]\left(V^2+\frac{\eta V^3 d}{10\sqrt{\Phi_0}}\right)\right\} \tag{13}$$

and

$$G_{(\mathrm{AP})}=\frac{2\pi e^2}{\hbar}\exp[-1.024d\sqrt{\Phi_0}] \times[N_m^F]^2\left\{2r\exp\left[\frac{\eta Vd}{2\sqrt{\Phi_0}}\right]+\frac{\beta(r+\lambda)}{3} \times\left[\frac{\eta dV^2}{4\sqrt{\Phi_0}}\exp\left[\frac{\eta Vd}{2\sqrt{\Phi_0}}\right]+V\left(\exp\left[\frac{\eta Vd}{2\sqrt{\Phi_0}}\right]-1\right)\right] -\beta^2\lambda\exp\left[\frac{3\eta Vd}{10\sqrt{\Phi_0}}\right]\left(V^2+\frac{\eta V^3 d}{10\sqrt{\Phi_0}}\right)\right\}. \tag{14}$$

The expressions above can be easily inverted to obtain the resistance, with the MR defined as

$$\frac{\Delta R}{R}=\frac{R_{\mathrm{AP}}-R_{\mathrm{P}}}{R_{\mathrm{AP}}}. \tag{15}$$

Note that the above definition is limited to 100%, since $R_{\mathrm{AP}}>R_{\mathrm{P}}$. In the limit $V\to 0$ we have approximately

$$G_{(\mathrm{P})}=\frac{2\pi e^2}{\hbar}\exp[-1.024d\sqrt{\Phi_0}][N_m^F]^2(1+r^2) \times\exp\left[\frac{\eta Vd}{2\sqrt{\Phi_0}}\right]$$

and

$$G_{(\mathrm{AP})}=\frac{2\pi e^2}{\hbar}\exp[-1.024d\sqrt{\Phi_0}] \times[N_m^F]^2(2r)\exp\left[\frac{\eta Vd}{2\sqrt{\Phi_0}}\right].$$

With the experimental value of $\Delta R/R$ at zero bias, we can easily obtain the ratio of the densities of states r at the Fermi level by

$$r=\frac{1}{1-\left.\frac{\Delta R}{R}\right|_{V=0}}+\sqrt{\frac{1}{\left(1-\left.\frac{\Delta R}{R}\right|_{V=0}\right)^2}-1}, \tag{16}$$

which does not depend on the barrier parameters. In turn, the barrier height Φ_0 and thickness d determine the absolute value of the resistance. Typical values used in our examples

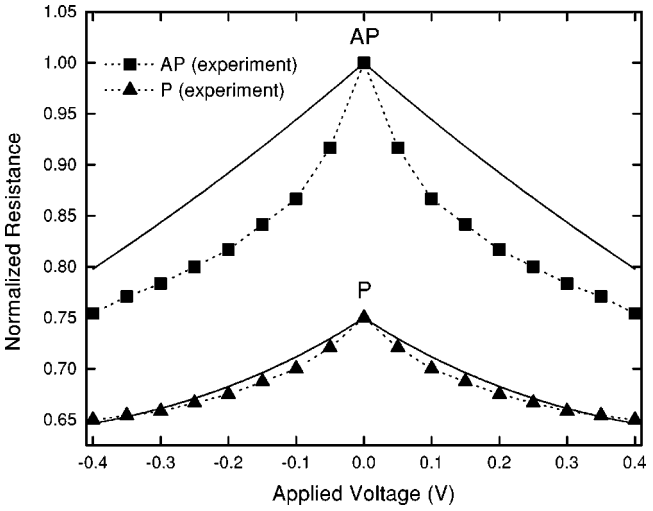

FIG. 1. Resistance as a function of the voltage bias for the AP and P configurations: the experimental results (dotted line and symbols) are taken from Ref. 8 and the theoretical ones (solid lines) are calculated with formulas (13) and (14), using the following parameters: $d=1.0$ nm. $\Phi_0=3.0$ eV, $N_m^F=1.0$ in normalized units, $r=2.21$, $\lambda=0.07$, $\beta=2.7$, and $\eta=0.1$. The resistances are given in arbitrary units, normalized to the peak value at zero bias.

are $d=1.0$ nm and $\Phi_0=3.0$ eV. Estimation of the resistance of such a junction yields resistance-area products of the order of $RS\approx 3.3\times 10^4\ [\Omega\,\mu\mathrm{m}^2]$, where S is the junction area given in $\mu\mathrm{m}^2$. This value follows closely the resistance-area scaling obtained for different junctions in Ref. 17, with values of the MR ranging from 16% to 22%. Representative experimental data of the tunneling resistance dependence on bias are given in Refs. 2, 3, 8, and 9. We compare our theoretical calculation with results presented in Ref. 8 at 4.2 °K. There, the *zero-bias* MR is approximately of the order of 25%, which yields for the r parameter of Eqs. (8) and (16) the value $r=2.21$. In Fig. 1 we show our theoretical results for the resistance calculated with formulas (13) and (14). The band structure parameters were taken with the values $\lambda=0.07$ and $\beta=2.7$, and the tunneling parameter as $\eta=0.1$. The small value of λ depicts a situation where the majority spin band is saturated at the Fermi level, while the minority one has a large variation.[10] However, the slope of the resistance near zero bias only depends on the ratio of the densities of states, in the form

$$R_{\mathrm{AP}}\approx R_0\left(\frac{1}{2r}-\frac{1}{2r}x\right), \qquad R_{\mathrm{P}}\approx R_0\left(\frac{1}{1+r^2}-\frac{1}{1+r^2}x\right), \tag{17}$$

where $x=\eta d|V|/(2\sqrt{\Phi_0})$ and $R_0=\exp[1.024d\sqrt{\Phi_0}]/(2\pi e^2/\hbar)[N_m^F]^2$ is a scale factor related to the absolute resistance. Note that we get a *zero bias anomaly*, but a good fit with the experiment is only obtained for the parallel configuration, as in Ref. 10. One can adequate the theoretical model to a better fit with the data, using more terms in the Taylor expansion of $W_{(C)}$, or leaving the densities of states as free parameters.[2] However, we interpret the failure of fitting the data for the AP configuration as a hint that points to the

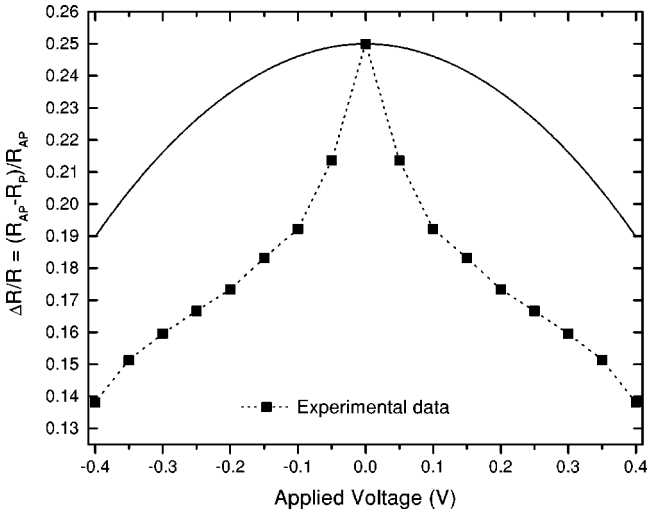

FIG. 2. Magnetoresistance as a function of voltage. Parameters are kept the same as in Fig. 1.

contribution of an extra mechanism, which affects differently the P and AP resistances. The linear terms in Eq. (17) cancel out when one gets the MR, as shown in Fig. 2, along with the experimental data. We pursue our argument further in the next section, with the inclusion of magnon inelastic scattering processes in the calculation of the MR.

IV. MAGNON-ASSISTED INELASTIC TUNNELING

In this section we consider not only the elastic (spin conserving) processes but inelastic magnon-assisted contributions to the tunneling current. The latter are responsible for opening the spin-flip channels, substantially reducing the MR near zero bias. Magnons are spin-wave excitations[16] which interact with electrons, being emitted or absorbed, thus producing changes in their energy and allowing for spin-flip scattering. Electrons accelerated by the electric field relax their energy, producing those collective excitations at the magnetic electrode interfaces. At low temperature, only magnon emission processes give a significant contribution to the resistance. However we analyze in the following the general case, describing each one of the eight processes associated with emission and absorption or magnons. There is one extra term related to the overlap between wave functions of the electrodes, not involving changes in the number of magnons. This term is proportional to the exchange transmission coefficient $T^J=|t^J_{kk'q}|^2$, resulting in a very similar formula to the one found for the direct tunneling in the previous section:

$$I^N_{(C)}=\frac{2\pi e}{\hbar}\int d\varepsilon (S_R^2+S_L^2)T^J(\epsilon,V,d,\Phi_0)W_{(C)}(\varepsilon,V)\times[f(\varepsilon-V)-f(\varepsilon)].$$

Let us consider now the electron tunneling from the left to the right electrode with the emission of one magnon at the right side interface

$$I^{E1}_{(C)}=\frac{2\pi e}{\hbar}\int d\omega\int d\varepsilon 2S_R T^J(\varepsilon,V,d,\Phi_0)\times N^L_{\downarrow}(\varepsilon-V+\hbar\omega)N^R_{\uparrow}(\varepsilon)\rho^{\mathrm{mag}}_R(\omega)[1+f_{\mathrm{BE}}(\omega)]\times f(\varepsilon-V+\hbar\omega)[1-f(\varepsilon)],$$

where $\rho^{\mathrm{mag}}(\omega)$ is the density of magnons at the right side interface and f_{BE} the Bose–Einstein distribution

$$f_{\mathrm{BE}}=\frac{1}{\exp\left[\dfrac{\hbar\omega}{k_BT}\right]-1}$$

An identical expression appears when considering the magnon emission at the left side interface yielding

$$I^{E1}_{(C)}=\frac{2\pi e}{\hbar}\int d\omega\int d\varepsilon 2[S_R\rho^{\mathrm{mag}}_R(\omega)+S_L\rho^{\mathrm{mag}}_L(\omega)]\times T^J(\varepsilon,V,d,\Phi_0)N^L_{\downarrow}(\varepsilon-V+\hbar\omega)\times N^R_{\uparrow}(E)[1+f_{\mathrm{BE}}(\omega)]f(\varepsilon-V+\hbar\omega)[1-f(\varepsilon)]. \quad (18)$$

When the tunneling occurs from right to left with one magnon emission, we have

$$I^{E2}_{(C)}=\frac{2\pi e}{\hbar}\int d\omega\int d\varepsilon 2[S_R\rho^{\mathrm{mag}}_R(\omega)+S_L\rho^{\mathrm{mag}}_L(\omega)]\times T^J(\varepsilon,V,d,\Phi_0)N^L_{\uparrow}(\varepsilon-V+\hbar\omega)N^R_{\downarrow}(\varepsilon)\times[1+f_{\mathrm{BE}}(\omega)]f(\varepsilon)[1-f(\varepsilon-V+\hbar\omega)]. \quad (19)$$

In turn, for magnon absorption we get

$$I^{A1}_{(C)}=\frac{2\pi e}{\hbar}\int d\omega\int d\varepsilon 2[S_R\rho^{\mathrm{mag}}_R(\omega)+S_L\rho^{\mathrm{mag}}_L(\omega)]\times T^J(\varepsilon,V,d,\Phi_0)N^L_{\uparrow}(\varepsilon-V-\hbar\omega)N^R_{\downarrow}(\varepsilon)\times[f_{\mathrm{BE}}(\omega)]f(\varepsilon-V-\hbar\omega)[1-f(\varepsilon)] \quad (20)$$

and

$$I^{A2}_{(C)}=\frac{2\pi e}{\hbar}\int d\omega\int d\varepsilon 2[S_R\rho^{\mathrm{mag}}_R(\omega)+S_L\rho^{\mathrm{mag}}_L(\omega)]\times T^J(\varepsilon,V,d,\Phi_0)N^L_{\downarrow}(\varepsilon-V-\hbar\omega)N^R_{\uparrow}(\varepsilon)\times[f_{\mathrm{BE}}(\omega)]f(\varepsilon)[1-f(\varepsilon-V-\hbar\omega)]. \quad (21)$$

The total current due to one magnon exchange is then

$$I_{\mathrm{mag}}=I^N_{(C)}+I^{E1}_{(C)}-I^{E2}_{(C)}+I^{A1}_{(C)}-I^{A2}_{(C)}. \quad (22)$$

Typical IET magnon spectra are shown by Ando and coworkers in Ref. 1. They display a strong peak around 12–20 mV and a rapid decrease for energies below the peak, due probably to a low energy cutoff, with a vanishing magnon density of states at very small energies. Introducing this low energy cutoff in the magnon spectrum, and taking the low temperature limit $T\to 0$ °K, we get $f_{\mathrm{BE}}\to 0$ for the Bose–Einstein distribution. This limit excludes the absorption terms in Eq. (22), leaving only the emission contributions to the total current

$$I_{\mathrm{mag}}=\frac{4\pi e}{\hbar}\int d\omega\int_0^{V-\hbar\omega}d\varepsilon\{T^J(\varepsilon,V,d,\Phi_0)[S_R\rho_R^{\mathrm{mag}}(\omega)+S_L\rho_L^{\mathrm{mag}}(\omega)]N_\downarrow^L(\varepsilon-V-\hbar\omega)N_\uparrow^R(\varepsilon)\Theta(V-\hbar\omega)-T^J(\varepsilon,V,d,\Phi_0)[S_R\rho_R^{\mathrm{mag}}(\omega)+S_L\rho_L^{\mathrm{mag}}(\omega)]\times N_\downarrow^R(\varepsilon)N_\uparrow^L(\varepsilon-V-\hbar\omega)\Theta(\hbar\omega-V)\}+I_{(C)}^N, \quad (23)$$

where $\Theta(x)$ is the step function.

One can use as the magnon dispersion relation a simple isotropic parabolic dependence, i.e., $\hbar\omega=E_m(q/q_m)^2$, where E_m is related to the Curie temperature by the mean field approximation $E_m=3k_BT_C/(S+1)$, and q_m is the radius of the first Brillouin zone.[8] In other words E_m is the maximum magnon energy (high energy cutoff).[1] Considering the above discussion, assuming identical ferromagnetic electrodes, and after some mathematical simplifications, one finally gets the conductance in the form

$$G_C=G_C^d+G_C^{\mathrm{mag}},$$

where G_C^d is given by Eqs. (13) and (14), for P and AP alignment, respectively, and G_C^{mag} is shown below

$$G_{\mathrm{P}}^{\mathrm{mag}}=\frac{2\pi e^2}{\hbar}T^j(V)[2S^2W_{(\mathrm{P})}+\Lambda(V)SW_{(\mathrm{AP})}], \quad (24)$$

and

$$G_{\mathrm{AP}}^{\mathrm{mag}}=\frac{2\pi e^2}{\hbar}T^J(V)[2S^2W_{(\mathrm{AP})}+2\Lambda(V)SW_{(\mathrm{P})}], \quad (25)$$

with $S=(S^R+S^L)/2$ and

$$\Lambda(V)=\begin{cases}V/E_m & \text{for } V<E_m,\\ 2-E_m/V & \text{for } V>E_m.\end{cases}$$

The functions $W_{(\mathrm{P})}$ and $W_{(\mathrm{AP})}$ in Eqs. (24) and (25) have been evaluated near zero bias, using formulas (9) and (10), respectively, substituting ε by the constant value 0.1 eV. We point out that magnon processes significantly contribute to the conductance only for voltages below 100 mV, and so we can consider $W_{(\mathrm{P})}$ and $W_{(\mathrm{AP})}$ as almost constant under the integration sign. The exchange tunneling coefficient T^J generally is one or two orders of magnitude smaller than the direct coefficient. We found excellent agreement between our theory and the experimental data using the same set of parameters of Fig. 1 for the tunneling barrier and the electronic structure, spin $S=3/2$ and $T^d/T^J=37$ for the ratio of the direct tunneling to the exchange tunneling coefficient. The magnon cutoff E_m was taken to be 90 meV. The results are shown in Fig. 3 for the resistances and in Fig. 4 for the corresponding MR. Clearly, the AP configuration is more sensible to the magnon contribution, since the current for that configuration is weighted by the product $N_M^IN_M^R$, which is much bigger than the factors $N_m^LN_M^R$ or $N_M^LN_m^R$ which appear in the P current, with the indices *m* and *M* referring to *minority* and *majority* spin bands (compare Figs. 1 and 3). Obviously, minor differences between theory and experimental data come from the fact that we are using a very simplified model for the band structure and the magnon dispersion relation. We comment on these results in the next section.

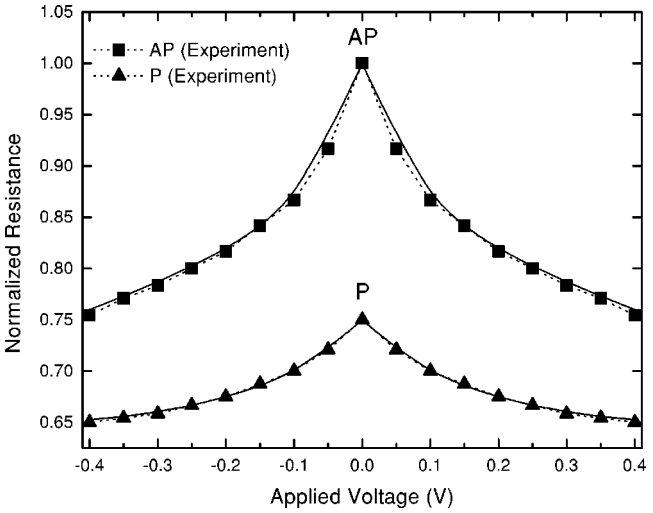

FIG. 3. Resistance, in arbitrary units, as a function of the voltage bias for the AP and P configurations: the experimental results (dotted line and symbols) are taken from Ref. 8 and the theoretical ones (solid lines) include magnon-assisted tunneling. Parameters are kept the same as in Fig. 1, with the addition of $T^d/T^J=37$.

V. CONCLUSIONS

We have presented a consistent study of the voltage dependence of the ''giant'' magnetoresistance in ferromagnetic tunneling junctions. Our approach includes: (a) lowering of the effective barrier height with the applied voltage; (b) different variations of the density of states for each spin band with voltage; and (c) magnon assisted inelastic tunneling near zero bias. We found that taking into account all those effects is essential to fully explain experimental results at low temperature for the voltage range between 0 and 500 mV. We have also clarified the role of the different parameters used in the theory: Some of them (d,Φ_0,η) determine the absolute value of the resistance at zero bias, which in turn is a scale factor in the theory; a different set, related to the band structure (r,β,λ), mainly monitors the global behavior with voltage and the value of the junction MR. To adjust our

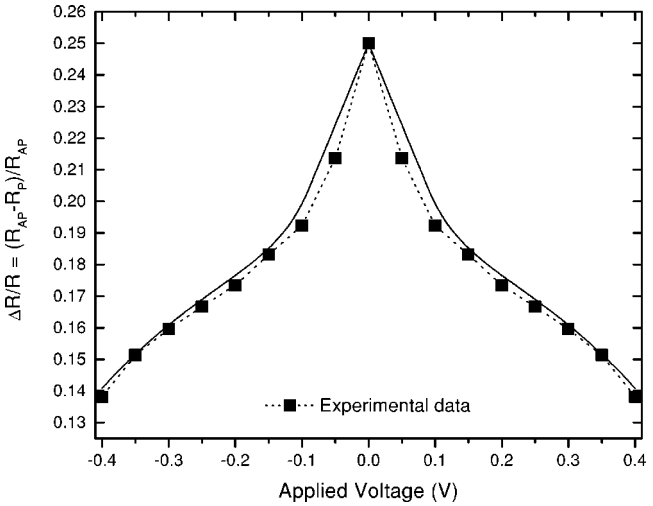

FIG. 4. Magnetoresistance as a function of voltage. Parameters are kept the same as in Fig. 3.

results with selected experimental data, we have taken β, $\lambda > 0$, but as shown in Ref. 10, this scenario is not unique and depends on the topology of the bands that contribute to the current; and finally, the behavior near zero bias (*zero bias anomaly*), with a rapid decrease of the resistance for the AP configuration up to 100 mV, is ascribed to magnon-assisted tunneling. Our estimation of $T^d/T^J \sim 40$ seems to be more realistic than previous estimations.[8] We note that the latter is the only adjustable parameter to fit the voltage dependence below 100 mV (for both P and AP configurations). Our calculation is in excellent agreement with the experimental data (see Figs. 3 and 4).

Temperature effects are not discussed in this article. As shown in Sec. IV, only magnon emission processes are included at low temperature ($T \to 0$). At finite temperature, we expect a decrease of the resistance near zero bias, due to one-magnon-absorption assisted tunneling.[18] The above should be superimposed to the thermal smearing in the Fermi–Dirac distribution of tunneling electrons.[3]

ACKNOWLEDGMENT

The authors would like to acknowledge partial financial support from *Fundaçao do Amparo à Pesquisa do Estado de São Paulo* (FAPESP, SP, Brazil), through Project No. 2002/09895-6.

[1] Y. Ando, J. Murai, H. Kubota, and T. Miyazaki, J. Appl. Phys. **87**, 5209 (2000).
[2] X. H. Xiang, T. Zhu, J. Du, G. Landry, and J. Q. Xiao, Phys. Rev. B **66**, 174407 (2002).
[3] J. J. Akerman, I. V. Roushchin, J. M. Slaughter, R. W. Dave, and I. K. Schuller, Europhys. Lett. **63**, 104 (2003).
[4] F. Montaigne, J. Nassar, A. Vaurès, F. Nguyen Van Dau, F. Petroff, A. Schuhl, and A. Fert, Appl. Phys. Lett. **73**, 2829 (1998).
[5] T. Miyazaki and N. Tezuka, J. Magn. Magn. Mater. **139**, L231 (1995).
[6] G. G. Cabrera and L. M. Falicov, Phys. Status Solidi B **61**, 539 (1974); Phys. Rev. B **11**, 2651 (1975).
[7] M. Jullière, Phys. Lett. A **54**, 225 (1975).
[8] S. Zhang, P. M. Levy, A. C. Marley, and S. S. P. Parkin, Phys. Rev. Lett. **79**, 3744 (1997).
[9] J. S. Moodera, J. Nowak, and R. J. M. van de Veerdonk, Phys. Rev. Lett. **80**, 2941 (1998).
[10] G. G. Cabrera and N. García, Appl. Phys. Lett. **80**, 1782 (2002).
[11] J. G. Simmons, J. Appl. Phys. **34**, 1793 (1963).
[12] M. Sharma, S. W. Wang, and J. H. Nickel, Phys. Rev. Lett. **82**, 616 (1999).
[13] P. LeClair, J. T. Kohlhepp, H. J. M. Swagten, and W. J. M. de Jonge, Phys. Rev. Lett. **86**, 1066 (2001).
[14] N. García, Appl. Phys. Lett. **77**, 1351 (2000).
[15] D. K. Ferry and S. M. Goodnick, *Transport in Nanostructures* (Cambridge University Press, Cambridge, 1997); Y. Imry, *Introduction to Mesoscopic Physics* (Oxford University Press, Oxford, 1997).
[16] D. C. Mattis, *The Theory of Magnetism* (Harper and Row Publishers, New York, 1965); C. Kittel, *Quantum Theory of Solids* (Wiley, New York, 1963).
[17] W. J. Gallagher, S. S. P. Parkin, Yu Lu, X. P. Bian, A. Marley, K. P. Roche, R. A. Altman, S. A. Rishton, C. Jahnes, T. M. Shaw, and Gang Xiao, J. Appl. Phys. **81**, 3741 (1997).
[18] C. A. Dartora and G. G. Cabrera (unpublished).